

# ANALYSIS AND DESIGN OF H-PLANE WAVEGUIDE BENDS WITH COMPACT SIZE, WIDE-BAND AND LOW RETURN LOSS CHARACTERISTICS

Zhewang Ma, Taku Yamane, and Eikichi Yamashita  
 University of Electro-Communications  
 1-5-1 Chofugaoka, Chofu-shi, Tokyo 182, Japan

## ABSTRACT

Accurate and efficient characterization method of compensated H-plane waveguide bends is developed by combining the port reflection coefficient method and the mode-matching method. Convergence properties and reliabilities of the obtained numerical results are verified. Variations of the return loss of three types of compensated bends are investigated with various compensation dimensions. Wide-band and low return loss bends with the obtained optimal compensation dimensions are fabricated and tested, and the measured results agree well with the theoretical predictions.

## INTRODUCTION

Waveguide bend is widely used in many composed waveguide components and subsystems, like power dividers, multiplexers, couplers and satellite beamforming networks [1]. In the design of waveguide bends, two objectives are most frequently considered as of paramount importance. One is the minimization of the return loss of the bend in a frequency band as wide as possible, and the other is the minimization of the size of the bend. To end these objectives, compensated waveguide bends are widely utilized.

A detailed, albeit not exhaustive, review of past publications on waveguide bends reveals that, most of the papers using the full-wave methods addressed primarily analytical and numerical techniques for achieving minimum approximations and maximum accuracy and efficiency in the treatment of compensated waveguide bends, and they contained little information concerning dimensioning rules for realizing compact-sized, wide-band and low return loss bends [1]-[8].

In this work, by combining the port reflection coefficient method [9] and the mode-matching method, we implement comparative studies of three types of compensated H-plane waveguide 90° right angle bends, as shown in Fig. 1. These waveguide bends are of small size and simple structure, without any additional matching elements, like septums or screws. This allows easier fabrication and thus smaller tolerance errors. With the

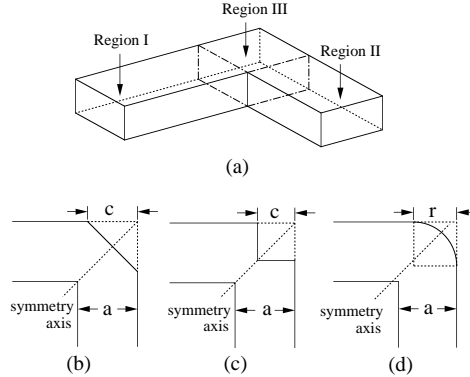


Figure 1: (a) An H-plane waveguide right angle corner bend, (b) a mitered bend, (c) a squarely cut bend, and (d) a circular bend.

obtained optimal compensation dimensions, wide-band and low return loss bends are theoretically predicted and experimentally realized.

## ANALYSIS METHOD

The general principle of the port reflection coefficient method (PRCM) for multi-port microwave networks was interpreted in [9]. In the case of a two-port network, it was found that if we can obtain three pairs of reflection coefficients  $R_1^{(i)}$  and  $R_2^{(i)}$  ( $i = 1, 2, 3$ ) at Port 1 and 2, we can solve  $S_{11}$  and  $S_{22}$  by using

$$S_{11} = [(R_1^{(1)}R_2^{(1)} - R_1^{(2)}R_2^{(2)})(R_1^{(1)} - R_1^{(3)}) - (R_1^{(1)} - R_1^{(3)})(R_1^{(1)} - R_1^{(2)})] / [(R_2^{(1)} - R_2^{(2)})(R_1^{(1)} - R_1^{(2)})] \quad (1a)$$

$$S_{22} = \frac{R_1^{(1)}R_2^{(1)} - R_1^{(2)}R_2^{(2)} - (R_2^{(1)} - R_2^{(2)})S_{11}}{R_1^{(1)} - R_1^{(2)}} \quad (1b)$$

For a reciprocal network,  $S_{12} = S_{21}$ , we have

$$S_{21} = \pm \sqrt{(S_{11} - R_1^{(1)})(S_{22} - R_2^{(1)})} \quad (2)$$

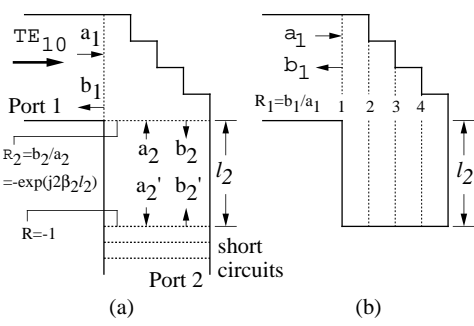


Figure 2: Calculation scheme of the reflection coefficients at Port 1 and 2.

In order to obtain the reflection coefficients at Port 1 and 2 of a waveguide bend in a convenient way, we place a short circuit at Port 2, and approximate the slanted or curvilinear part of the bend by a staircase, as shown in Fig. 2(a). Then the reflection coefficient at Port 2 can be obtained in advance by using

$$R_2 = -e^{j2\beta_2 l_2} \quad (3)$$

here  $\beta_2$  is the phase constant of the operating mode at Port 2, and  $l_2$  is the distance between the short circuit and the discontinuity region. On the other hand, the reflection coefficient  $R_1$  at Port 1 can be now easily computed by using the full-wave mode-matching method, together with the generalized scattering matrix technique. This is because after the termination of Port 2 by a short circuit, the analyzed structure can be viewed, looking from Port 1, as a one-port structure comprised of cascaded waveguide step-junctions only, as illustrated in Fig. 2(b).

Repeating the above calculation process three times by moving the short circuit at Port 2 with different positions, we get three pairs of reflection coefficients at Port 1 and 2. Substituting the obtained reflection coefficients into (1) and (2), we get the desired scattering parameters of the compensated bend.

Higher order modes excited around the corner region have been taken into consideration in the mode-matching treatment of the step-junctions. Also the generalized scattering matrix technique is used for connecting the cascaded step-junctions. Therefore, the obtained results are accurate full-wave solutions.

## NUMERICAL RESULTS

In Figs. 3(a) and (b), the calculated scattering parameters of a mitered and a circular bend are shown with different numbers of division steps used in the staircase approximation of the slanted or circular part of the bend. The results obtained by the boundary-element method (BEM) [3] are also drawn in Fig. 3(a)

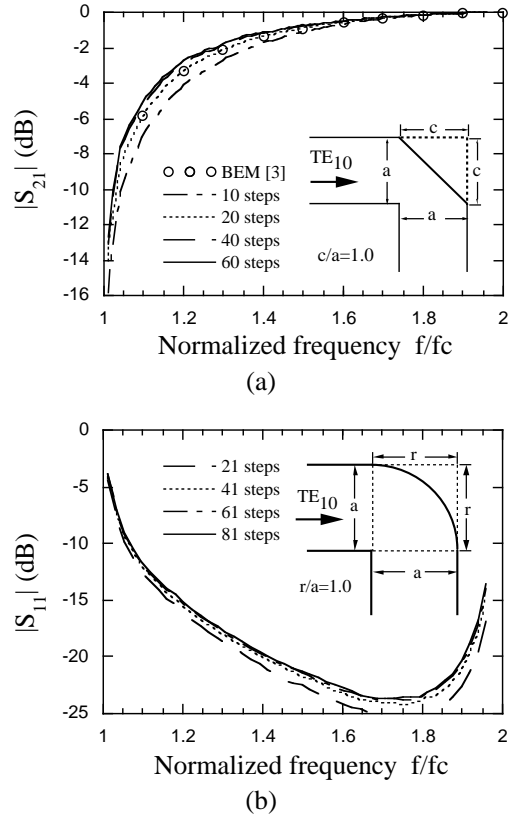


Figure 3: Variation of the scattering parameters of a mitered and a circular bend with different numbers of steps used in the staircase approximation.

for comparison. It is seen that when the number of steps is greater than 40, converged results are guaranteed. When 60 steps are used in the approximation, the calculation time of each frequency point is about 20 seconds on a SUN SPARC server 1000 workstation.

Chan et al. [10] reported that staircase approximation of curvilinear boundaries in the FDTD method may yield converged but unreliable results. They found that even a large number of steps are used in the approximation, a slight displacement of two or four steps may cause quite large variation of the results. Since our numerical results are obtained with a staircase approximation of the compensated part, the reliability of the results is verified here by using the method of [10]. As shown by the dashed lines in Fig. 4, among the many steps used in the staircase approximation, we move four arbitrary steps by half a step and recalculate the scattering parameters of the bend. The steps can be displaced inwards or outwards, and in Figs. 4(a)-(d) we illustrated four choices of displacement used in our verification. The difference between the results obtained with and without the displacement of the steps is shown in Fig. 5. It is seen that with the increase of the number of steps, the difference becomes smaller and smaller. This suggests

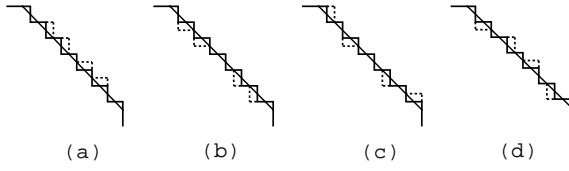


Figure 4: Displacement of steps for the verification of the reliabilities of the results.

that stable and reliable results are guaranteed when the number of steps used for the staircase approximation is large enough.

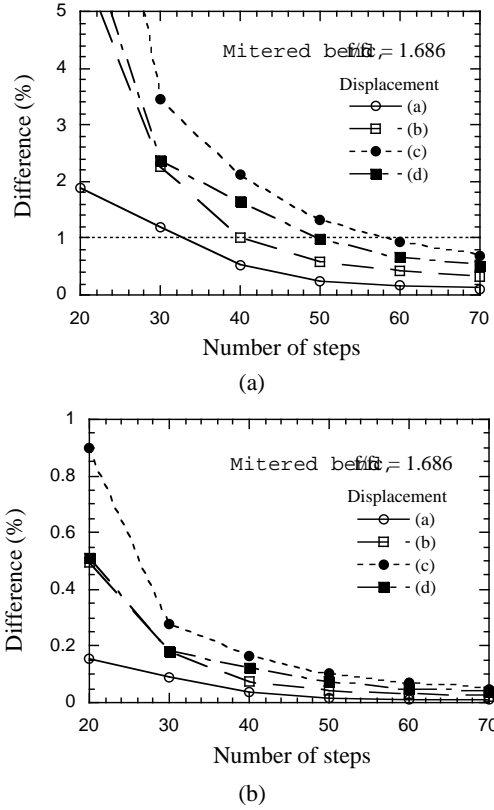


Figure 5: Difference between the scattering parameters of a mitered bend calculated with and without the displacement of steps. (a)  $S_{11}$ , (b)  $S_{21}$ .

Variations of the return loss of the three types of bends with various dimensions of the compensated parts are shown in Figs. 6-8. In the case of the mitered bend, the low return loss ( $|S_{11}| < -30$  dB) frequency band is available when  $0.61 \leq c/a \leq 0.76$ . The optimal compensation dimension is  $c/a=0.631$ , at which the low return loss bandwidth reaches approximately 39%. In the case of the squarely cut bend, the low return loss frequency band is available when  $0.34 \leq c/a \leq 0.45$ . The optimal compensation dimension is  $c/a=0.347$ , at which

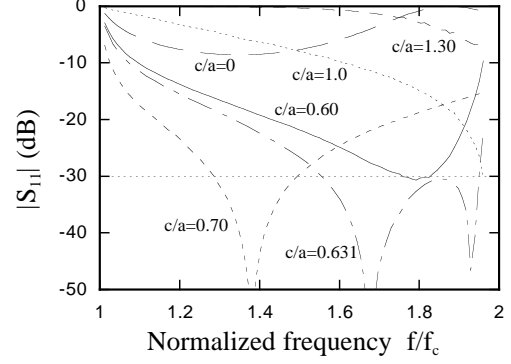


Figure 6: Variation of the return loss of a mitered bend with various dimensions of the mitered part.

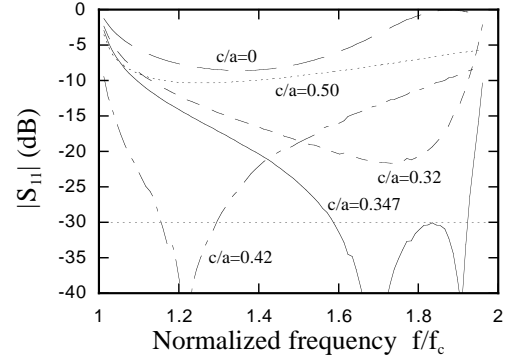


Figure 7: Variation of the return loss of a squarely cut bend with various dimensions of the cut part.

the low return loss bandwidth is about 33%. In the case of the circular bend, the low return loss frequency band is available when  $1.10 \leq c/a \leq 1.5$ . When  $r/a=1.18 \sim 1.20$ , the return loss is less than  $-30$  dB over the whole single mode frequency band.

Based on the obtained optimal compensation dimensions, three types of H-plane waveguide bends are designed and fabricated. The dimensions of the waveguide used are  $a=19.050$  mm and  $b=9.525$  mm, and the measurement is made in the frequency range  $10 \sim 15$  GHz. The calculated and measured return loss of the squarely cut bend are compared in Fig. 9. The solid line indicates the calculated result of the bend with the optimal compensation dimension  $c/a=0.631$ . However, the actual dimension of the fabricated bend is  $c/a=0.636$  because of the fabrication error of 1 mm. The return loss of the bend is recalculated using the actual dimension  $c/a=0.636$ , and the result is plotted in Fig. 9 by the dotted line. It agrees very well with the measured data over the whole frequency band.

The calculated and measured return loss of the circular bend are compared in Fig. 10. It is seen that over the whole frequency band, the measured return loss is of the level of  $-35$  dB. There is a small discrepancy between the theoretical and measured values. This is reasonable

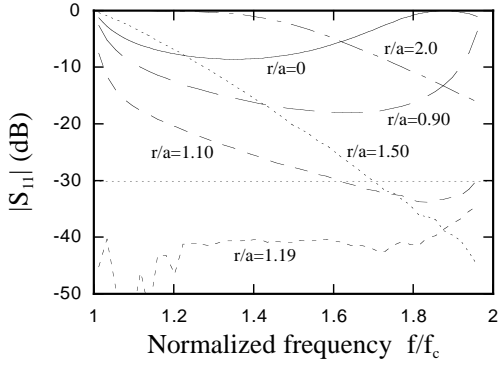


Figure 8: Variation of the return loss of a circular bend with various radii of the circular part.

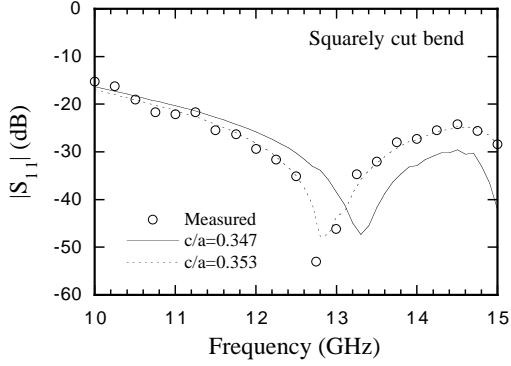


Figure 9: Comparison between the calculated and measured return loss of a squarely cut bend.

because a return loss of the level of  $-40$  dB is actually quite small and is thereby difficult to be measured precisely. Moreover, in the measurement a matching-load with a return loss of  $-40$  dB or less is used, and this will surely introduce additional measurement errors. Therefore, the agreement between the calculated and measured results can be say good. Above all, a full-band matched bend is theoretically predicted and experimentally realized by using this simple circular structure, which is smaller than most previously reported curved bends because the inner side of the circular bend here is a sharp  $90^\circ$  angle corner.

## ACKNOWLEDGMENT

The authors thank Dr. M. Miyazaki of the Mitsubishi Electric Corporation for his helpful discussions.

## REFERENCES

- [1] J. Uher, J. Bornemann, and Uwe Rosenberg, *Waveguide Components for Antenna Feed Systems: Theory and CAD*. Boston: Artech House, 1993.
- [2] N. Marcuvits, *Waveguide Handbook*. vol. 10, Radiation Laboratory Series. New-York: McGraw-Hill, 1951.
- [3] M. Koshiba and M. Suzuki, "Application of the boundary-element method to waveguide discontinuities," *IEEE Trans. Microwave Theory Tech.*, vol. MTT-34, pp. 301-307, Feb. 1986.
- [4] J. M. Reiter and F. Arndt, "Rigorous analysis of arbitrary shaped *H*- and *E*-plane discontinuities in rectangular waveguides by a full-wave boundary contour mode-matching method," *IEEE Trans. Microwave Theory Tech.*, vol. MTT-43, pp. 796-801, Apr. 1995.
- [5] F. Alimenti, M. Mongiardo, and R. Sorrentino, "Design of mitered *H*-plane bends in rectangular waveguides by combined mode matching and finite differences," *Proc. 24th European Microwave Conf.*, Sept. 1994, pp. 289-293.
- [6] F. Monglie, T. Rozzi, and P. Marozzi, "Wideband matching of waveguide discontinuities by FDTD methods," *IEEE Trans. Microwave Theory Tech.*, vol. MTT-42, pp. 2093-2098, Nov. 1994.
- [7] M. Mongiardo, A. Morini, and T. Rozzi, "Analysis and design of full-band matched waveguide bends," *IEEE Trans. Microwave Theory Tech.*, vol. MTT-43, pp. 2965-2971, Dec. 1995.
- [8] F. C. de Ronde, "Full-band matching of waveguide discontinuities," *IEEE MTT-S Int. Microwave Symp. Dig.*, Palo Alto, CA, 1966.
- [9] Z. Ma and E. Yamashita, "Port reflection coefficient method for solving multi-port microwave network problems," *IEEE Trans. Microwave Theory Tech.*, vol. MTT-43, pp. 331-337, Feb. 1995.
- [10] C. H. Chan, H. Sangani, K. S. Yee, and J. T. Elson, "A finite-difference time-domain method using Whitney elements," *Microwave and Optical Technology Letters.*, vol. 7, no. 14, pp. 673-676, Oct. 1994.

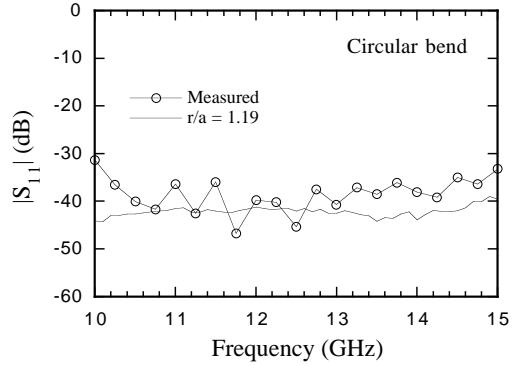


Figure 10: Comparison between the calculated and measured return loss of a circular bend.